

Higgs self coupling measurement in e^+e^- collisions at center-of-mass energy of 800 GeV

P. Gay

Laboratoire de Physique Corpusculaire, Univ. B. Pascal/IN²P³-CNRS, 24 Av. des Landais, F-63177 Aubière Cedex, France

Abstract. Feasibility of the measurement of the trilinear self-coupling of the Higgs boson is studied at centre of mass energy of 800 GeV. Double-Higgs strahlung as well as WW fusion processes has been investigated with a realistic simulation of a typical detector. With the combination of the two processes, the self Higgs coupling may be measured with a 14 % precision when an integrated luminosity of 2 ab^{-1} would be collected at the Linear Collider.

Keywords. Higgs, trilinear coupling, Linear Collider

PACS Nos 2.0

1. Introduction

In the framework of the standard model, the generation of mass occurs through the Higgs mechanism. This mechanism assumes a Higgs potential which behaves as $\lambda(\Phi^2 - \frac{1}{2}v^2)^2$, where ϕ is an isodoublet scalar field, and $v \sim 246 \text{ GeV}$ is the vacuum expectation value of its neutral component. Measurement of the trilinear self-coupling $\lambda_{\text{hhh}} = \frac{6}{\sqrt{2}} \lambda v$ offers an independent determination of the Higgs potential shape and a direct experimental test of the Higgs mechanism. A feasibility of the measurement of self Higgs coupling has already been performed at center-of-mass energy of 500 GeV. A new analysis has been performed at a higher centre-of-mass energy of 800 GeV, in order to include the WW-fusion process.

2. Simulation and analysis

The trilinear Higgs self-coupling could be extracted from the measurement of the cross-section of each of the following processes : double Higgs-strahlung ($e^+e^- \rightarrow Zhh$) or WW double-Higgs fusion ($e^+e^- \rightarrow \bar{\nu}_e \nu_e hh$) [1]. Feynman diagrams involved are indicated on Fig. 1 and 2.

At centre-of-mass energy around 500 GeV the double Higgs-strahlung is dominant with respect to WW fusion one but at centre-of-mass energy close to 800 GeV, the WW fusion is more important. The study presented here will be performed for $m_h = 120 \text{ GeV}/c^2$ and $\sqrt{s} = 800 \text{ GeV}$ in the standard model framework. With an expected integrated luminosity

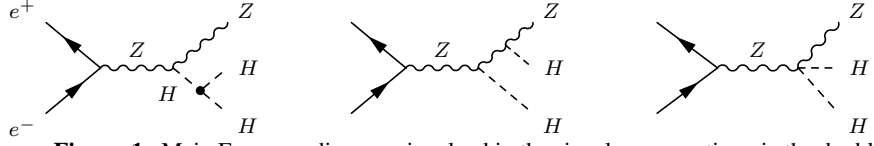


Figure 1. Main Feynman diagrams involved in the signal cross-section via the double Higgs-strahlung.

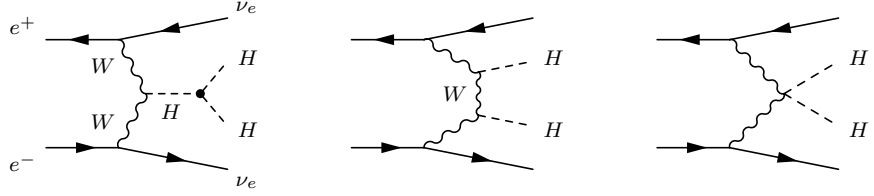


Figure 2. Main Feynman diagrams involved in the signal cross-section via the WW fusion.

of 500 fb^{-1} , the number of events expected from the signal is only of 90 events, while the background processes yield to an sample of events which is greater by many order of magnitude. Only part of the diagrams involve self Higgs coupling and sample of events corresponding to those diagrams have been simulated in order to evaluate the efficiencies of the analysis to that particular contribution from double-Higgsstrahlung and WW-fusion processes. For light Higgs boson masses, the Higgs boson decays predominantly in $b\bar{b}$ pair and the signature of those final states is characterised by multijet environment with a high b -like content with or without missing energy. The signal and background event samples have been simulated with the WHIZARD generator [3] and PYTHIA [4] has been used to perform the hadronisation of the primary parton. The CIRCE package [2] has been used to introduce the initial energy dispersion. The background sources are either four and six fermions final state processes. The following processes $e^+e^- \rightarrow W^+W^-$, ZZ , hZ and $e^+e^- \rightarrow WWZ$, ZZZ have been simulated. In order to take into account the diffusion at low angle dedicated samples have been generated for $e^+e^- \rightarrow We\nu$, Zee , $WW\nu\bar{\nu}$, ZZe^+e^- , $ZZ\nu\bar{\nu}$ and $ZWe\nu$ processes. The top pair production, which leads to six fermions final state has been simulated as well as $e^+e^- \rightarrow t\bar{t}h$, $t\bar{t}Z$. A dedicated sample of $e^+e^- \rightarrow t\bar{t}\nu\bar{\nu}$ has been generated. Table 1 summaries the size of the samples used and the cross-section of each process. The detector simulation was performed with a Parametric Monte Carlo [5]. The tracking system consists on a vertex detector (VDET) surrounding the beam tube followed by a time projection chamber (TPC). The tracking system is complemented with a forward tracker and muon chambers. The hermeticity of the detector is reinforced at low angle with a luminometer (LCAL). Energy and direction of the photons and neutral hadrons are measured thanks to the electromagnetic (ECAL) and hadronic (HCAL) calorimeters with an energy resolutions of $\Delta E/E=10.2\%/\sqrt{E(\text{GeV})}$ and $\Delta E/E=40.5\%/\sqrt{E(\text{GeV})}$ respectively for ECAL/LCAL and HCAL. Smearred clusters in calorimeters and smearred tracks are combined in order to form the best reconstructed objects so-called here after *eflow* objects. The selection is split in two branches according the value of total visible energy (E_{vis}) measured in the detector. This energy is defined from the *eflow* reconstructed objects. Selection (A) corresponds to the events where E_{vis} is greater than 500 GeV. The event is therefore forced in six jets with the DURHAM scheme. Selection (B) collected the

Table 1. Cross-sections of the processes, Monte Carlo statistics and simulated luminosity (\mathcal{L}_{sim}). Numbers of events expected from signal (S_{hhh}), background processes (B_{tot}) and contribution for selection A and B (resp. N_{selA} and N_{selB}). Relative error ($\Delta\lambda/\lambda$) on λ for selection (A) and (B) and an 2 ab^{-1} integrated luminosity. The signal number of event (S_{hhh}) and signal efficiency (ϵ_{hhh}) corresponds to the sub-sample of events involving hhh coupling.

process	N_{gen}	σ (fb)	$\mathcal{L}_{sim}(\text{fb}^{-1})$	N_{selA}		N_{selB}
				loose cut	tight cut	
signal	10k	0.1844	54227			
WW	9.2M	668.8	13890	-		
ZZ	1.5M	222.4	6744	32.6		1.48
hZ	160k	22.65	7064.	64.3		5.64
t \bar{t}	1M	260.	3840.	391.		
t \bar{t} h	20k	2.498	8006	69.3	10.5	
t \bar{t} Z	25k	4.528	5521	40.6	7.24	
t \bar{t} $\nu\bar{\nu}$	20k	0.787	25400.	0.16		
WWZ	100k	56.96	1755.	1.12		
ZZZ	25k	0.729	34280.	10.9	4.12	
WW $\nu\bar{\nu}$	60k	12.43	4827.	-		
ZZe $^+e^-$	3k	0.287	10400.	1.72		
ZZ $\nu\bar{\nu}$	25k	3.477	7190.	0.28		1.96
ZWe ν	12k	10.09	1176.	-		
			B_{tot}	612.	21.3	9.1
			S_{hhh}	137.6	88.	34.
			ϵ_{hhh}	42.6%	30.2%	37.3%
			$s/\sqrt{s+b}$	5.	8.2	5.2
			$\Delta\lambda/\lambda$		21.7%	17.6%

events with E_{vis} less 500 GeV, and forced into four jets. In a second part, combination of the di-jets reconstructed masses are used to reject the three-bosons and di-bosons final-state contribution taking advantage of the reconstruction of two Higgs bosons. The flavour tagging will play an important rôle. The b-tagging and c-jet contamination is performed through a parametrisation derived from full reconstruction [6]. Finally, relevant informations are combined with a multivariable method (neural network) as illustrated on Fig. 3 for the six jets topology.

The contribution from the various background sources are reported in Table 1 for the selection (A) with the loose and tightened cuts and for the selection (B). The signal efficiencies are 30.2% and 37.3% respectively for the selection (A) and (B). Those efficiencies are derived from a sample of signal events generated with only diagramma involving the trilinear hhh coupling in the cross-section. Assuming an integrated luminosity of 2000fb^{-1} the combination of the two selections leads to 30.4 events expected from background processes and 122 events from the signal sensible to the hhh coupling.

3. Conclusion

To establish the Higgs mechanism in an unambiguous way, the self-energy potential of the Higgs field must be reconstructed. This implies the determination of the trilinear self-

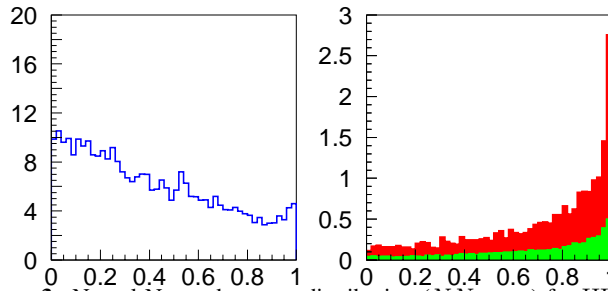


Figure 3. Neural Network output distribution (NN_{output}) for HHZ signal (full histogram) and background (empty histogram) with 500 fb^{-1} and $m_h=120 \text{ GeV}/c^2$.

coupling. The experimental feasibility of the measurement has been explored through a detailed analysis of the reconstruction of the double Higgs-strahlung and W-Wfusion events. To derive the relative error on λ_{hhh} the relation between λ_{hhh} and the cross-section has to be taken into account and the relative error on the trilinear Higgs coupling ($\Delta\lambda/\lambda$) is displayed on Table 1 for an integrated luminosity of 2 ab^{-1} . With the same integrated luminosity, the combination of the two analysis indicated that a relative error on λ_{hhh} of 14% may be achieved.

References

- [1] A. Djouadi, W. Killian, M. Muhlleitner and P. Zerwas, Eur. Phys. J. C10; P. Osland, P.N. Pandita, Phys. Rev. D ; D.J. Miller and S. Moretti RAL-TR-99-032, May 1999
- [2] T. Ohl, Comput.Phys.Commun.101:269-288,1997 [hep-ph/9607454]
- [3] W. Kilian, LC-TOOL-2001-039 (available from <http://www-flc.desy.de/lcnotes/>)
- [4] T. Sjöstrand, High-energy-physics event generation with PYTHIA 5.7 and JETSET 7.4, Compt. Phys. Commun.82 (1994) 74
- [5] M. Pohl, H.J. Schreiber, SIMDET.3 A Parametric Monte Carlo for a TESLA Detector, DESY 99-030 (1999)
- [6] R. Hawkings, Vertex detector and flavour tagging studies for the TESLA linear collider, LC-PHSM/2000-026